# A Robust Estimation Algorithm for Printer Modeling*

Mario Rotea and Carlos Lana

***Abstract*— This paper describes a robust estimation algorithm (REA) for estimating the device-specific parameters of the so-called spectral Neugebauer model. This physics-based model is used to characterize the response of color printers. The various steps required to use REA are given. A detailed case study, using a high-end color printer, was conducted to evaluate the performance of REA relative to the methods of least squares and total least squares. The main result of the study shows that the model obtained with REA achieves the smallest approximation errors in both spectral and $L^*a^*b^*$ color spaces.**

## I. Introduction

Printer calibration plays a central role in print quality assurance. Calibration is necessary to guarantee that a given printer will consistently output the correct colors, despite aging and toner variations. Quantitative printer models are required in most printer calibration methods [1], [2]. These quantitative models are then inverted so that the printer's digital control values (e.g., cyan, magenta, yellow, and black) can be calculated as a function of the desired output color.

Approaches for printer modeling can be grouped in two categories: model-based approaches and empirical or interpolation-based approaches. The interpolation-based approaches have the potential of being more accurate if a large enough number of experiments is available [3], [4]. In contrast, the model-based approaches take advantage of the physics behind the process to achieve accuracy, especially in areas of the color space where experimental data is sparse [5], [6], [7], [1]. The model-based approach is the preferred approach when, due to cost and time constraints, the number of experiments available for tuning the model is limited.

References [8] and [9] have introduced a robust estimation algorithm (REA) for estimating the parameters of a physics-based model referred to as the spectral Neugebauer model [10]. This model takes as input the digital control values $CMYK$, which encode the desired amount color toners to be placed on the paper, and returns the spectral reflectance of the printed patch. The device-specific parameters of the Neugebauer model are determined from spectral measurements of the printed colors.

The fundamental advantage of REA relative to other techniques for parameter estimation, such as least squares and total least squares [1], is that the models generated with REA tend to be less sensitive to inevitable spatial nonuniformities and color drifts that arise depending on when and where on the paper the measurements are taken. On the other hand, REA is more elaborate and requires prior information on the uncertainty associated with the measurements in order to produce models with higher levels of robustness.

A block diagram of the spectral Neugebauer model is shown in Fig. 1. The equations associated with each block in the diagram are given in section II. The device-specific parameters are the four nonlinear mappings referred to as the dot-growth functions, and the primary reflectances which are used in the so-called Neugebauer equation indicated in Fig. 1. REA estimates these parameters by minimizing the largest worst-case spectral approximation error over a set of training experiments. For a given experiment, the worst-case approximation error is the maximal difference between the model output and the set of all reflectances obtained by perturbing the measured reflectance with an unknown but bounded perturbation. This bounded perturbation models measurement errors and modeling uncertainty. In theory, the model generated by REA is less susceptible to variations in the data than the models obtained with least-squares and total-least squares.

The present paper describes the robust estimation algorithm REA introduced in [8] and [9]. The data and steps required to execute the algorithm are explained in detail. The results of a case study using a high-end xerographic printer are also presented. A detailed comparison of the approximation errors in both spectral space and $L^*a^*b^*$ color space suggests that the models generated with REA outperform the models obtained with the methods of least squares and total least squares.

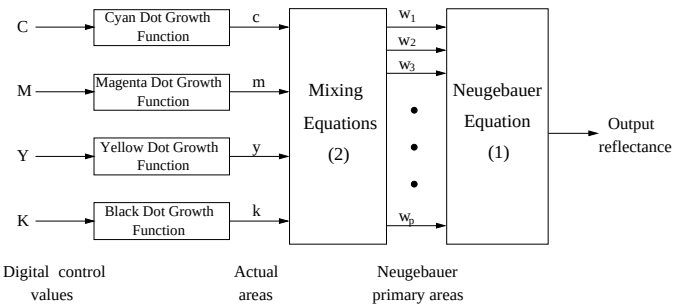


Fig. 1. Block diagram of the spectral Neugebauer model.

*Work supported in part by a Xerox Foundation University Affairs Committee Grant and in part by the National Science Foundation Grant ECS #0080832.

Mario Rotea is with the School of Aeronautics and Astronautics, 315 N. Grant Street, Purdue University, West Lafayette, IN 47907.

Carlos Lana is a PhD student in the School of Aeronautics and Astronautics, 315 N. Grant Street, Purdue University, West Lafayette, IN 47907.

*Notation*

| | |
|---|---|
| $r_o$ | True (unknown) reflectance |
| $\hat{r}$ | Model output reflectance |
| $\hat{r}_P$ | Model primary reflectance |
| $r$ | Measured reflectance |
| $r_C$, $r_M$, $r_Y$, $r_K$ | Cyan, magenta, yellow, and black single colorant measured reflectances |
| $C$, $M$, $Y$, $K$ | Cyan, Magenta, Yellow, and Black digital control values |
| $c$, $m$, $y$, $k$ | Cyan, magenta, yellow and black nondimensional actual areas |
| $n$ | Yule-Nielsen correction factor |
| $w$ | Neugebauer area |
| $\lambda$ | Wavelength |
| $\sigma$ | Reflectance error bound |
| $\lvert\cdot\rvert$ | Entry-wise absolute value for sequences |
| $\|x\|_2 = \sqrt{\sum_{k=1}^{N} x_k^2}$ | $\ell_2$ norm of the sequence $x = (x_1, \ldots, x_N)$ |

## II. The Neugebauer Printer Model

Four-colorant printers may be modeled by the following spectral Neugebauer equation [11], [10]

$$\hat{r}(\lambda) = \left\{ \sum_{i=1}^{16} w_i \hat{r}_{P,i}^{1/n}(\lambda) \right\}^n \tag{1}$$

where $\hat{r}(\lambda)$ is the output reflectance predicted by the model at wavelength $\lambda$, $w_i \geq 0$ represents the so-called Neugebauer primary area, $\hat{r}_{P,i}(\lambda)$ denotes the $i^{\text{th}}$ primary reflectance, and the number $n$ is the Yule-Nielsen correction factor.

For printers using rotated halftone screens, the Neugebauer areas $w_i$ can be modeled with the following equations

$$\begin{aligned}
w_1 &= (1-c)(1-m)(1-y)(1-k) && \text{(2a)}\\
w_2 &= c(1-m)(1-y)(1-k) && \text{(2b)}\\
w_3 &= (1-c)m(1-y)(1-k) && \text{(2c)}\\
w_4 &= (1-c)(1-m)y(1-k) && \text{(2d)}\\
w_5 &= (1-c)(1-m)(1-y)k && \text{(2e)}\\
w_6 &= cm(1-y)(1-k) && \text{(2f)}\\
w_7 &= c(1-m)y(1-k) && \text{(2g)}\\
w_8 &= c(1-m)(1-y)k && \text{(2h)}\\
w_9 &= (1-c)my(1-k) && \text{(2i)}\\
w_{10} &= (1-c)m(1-y)k && \text{(2j)}\\
w_{11} &= (1-c)(1-m)yk && \text{(2k)}\\
w_{12} &= cmy(1-k) && \text{(2l)}\\
w_{13} &= cm(1-y)k && \text{(2m)}\\
w_{14} &= c(1-m)yk && \text{(2n)}\\
w_{15} &= (1-c)myk && \text{(2o)}\\
w_{16} &= cmyk && \text{(2p)}
\end{aligned}$$

where $c, m, y$ and $k$ are the nondimensional areas occupied by cyan, magenta, yellow and black toner, respectively. These nondimensional areas are determined by the digital control values $C, M, Y$ and $K$, which are nondimensional integers from 0 to 255. Equations (2) are known as the Demichel equations [12].

Figure 1 depicts the input-output printer model composed by equation (1), the Demichel equations (2), and the dot growth functions $C \mapsto c, M \mapsto m, Y \mapsto y$, and $K \mapsto k$. For the model to be fully specified the following parameters must be known:

i) the dot growth functions $C \mapsto c, M \mapsto m, Y \mapsto y$, and $K \mapsto k$;
ii) the model primary reflectances $\hat{r}_{P,1}(\lambda), \ldots, \hat{r}_{P,16}(\lambda)$;
iii) the Yule-Nielsen factor $n$.

Section III explains the algorithm proposed in [8] and [9] for estimating these device-specific parameters.

## III. The Robust Estimation Algorithm (REA)

The fundamental concept behind REA is the worst-case approximation error in spectral space, which is defined as

$$E_{\text{worst}} = \max_{r_o} \|\hat{r} - r_o\|_2 \tag{3}$$

In this equation, $\hat{r} = (\hat{r}(\lambda_1), \hat{r}(\lambda_2) \ldots, \hat{r}(\lambda_N))$ is a sequence of output reflectances with components $\hat{r}(\lambda_k)$ calculated from (1), in response to a digital control input $CMYK$. The maximization in (3) is over all reflectances $r_o$ that satisfy the following inequality

$$|r_o(\lambda_k) - r(\lambda_k)| \leq \sigma(\lambda_k) \tag{4}$$

for all wavelengths $\lambda_k$, $k = 1, \ldots, N$, where $r(\lambda_k)$ is the measured output reflectance for the $CMYK$ digital control input, and $\sigma(\lambda_k)$ is a given sequence. Essentially, if $r_o(\lambda_k)$ satisfies (4) then it differs from the measured reflectance $r(\lambda_k)$ by no more than $\sigma(\lambda_k)$. The reflectance $r_o$ is interpreted as the true, but unknown, reflectance. The difference between $r_o$ and $r$ is due to the inherent modeling inaccuracy and the actual measurement errors. The sequence $\sigma(\lambda_k)$ is a bound on the size of this difference at each wavelength. The approximation error $E_{\text{worst}}$ in (3) is the largest difference between the model output reflectance $\hat{r}$ and the set of reflectances $r_o$ that satisfies the error bound in the inequality (4). It has been shown in [8] that the worst-case error may be computed from the simple expression

$$E_{\text{worst}} = \| \, |\hat{r} - r| + \sigma \|_2 \tag{5}$$

Ideally, one would like to determine the parameters of a spectral Neugebauer model that minimize the largest worst-case approximation error $E_{\text{worst}}$ over a set of experiments that span the entire printer gamut. That is, given the $P$ measured reflectance sequences $r_j = (r_j(\lambda_1), r_j(\lambda_2) \ldots, r_j(\lambda_N))$, $j = 1, \ldots, P$, then the model parameters are obtained by solving the following optimization

$$\min \max_{1 \leq j \leq P} \| \, |\hat{r}_j - r_j| + \sigma_j \|_2 \tag{6}$$

where $\hat{r}_j$ is the model reflectance computed with (1) and (2). The outer minimization in (6) is over the model parameters, which are: the four dot growth functions $C \mapsto c$, $M \mapsto m$, $Y \mapsto y$, and $K \mapsto k$, the 16 primary reflectances $\hat{r}_{P,1}$, …, $\hat{r}_{P,16}$, and the Yule-Nielsen correction factor $n$.

The ideal minimization problem defined in equation (6) is non-convex, with local optima that may not be global.

Reference [9] has given an algorithm to compute a suboptimal solution to this problem by splitting it into two simpler problems: the estimation of the dot growth functions and the estimation of the corrected primary reflectances, both problems with constant $n$. These problems are simpler because they do not involve products amongst the optimization variables. The algorithm introduced in [9] is the so-called robust estimation algorithm (REA), which makes use of the following experimental data.

### A. Experimental Data

*Primary reflectances:* The measured primary reflectance sequences are denoted by

$$r_{P,j} = (r_{P,j}(\lambda_1), \ldots, r_{P,j}(\lambda_N)) \tag{7}$$

where $j = 1, \ldots, 16$, indexes the specific reflectance and $\lambda_1$, ..., $\lambda_N$, are the wavelengths of interest. These sixteen output reflectances are obtained in response to all 16 possible combinations of digital control inputs $C$, $M$, $Y$, $K$ where each control value is either 0 or 255.

*Responses to single colorant inputs:* The measured output reflectance sequences in response to a set of single colorant digital control values $C$, $M$, $Y$, $K$, are denoted by

$$\begin{aligned} r_{C,j} &= (r_{C,j}(\lambda_1), \ldots, r_{C,j}(\lambda_N)) && \text{(8a)} \\ r_{M,j} &= (r_{M,j}(\lambda_1), \ldots, r_{M,j}(\lambda_N)) && \text{(8b)} \\ r_{Y,j} &= (r_{Y,j}(\lambda_1), \ldots, r_{Y,j}(\lambda_N)) && \text{(8c)} \\ r_{K,j} &= (r_{K,j}(\lambda_1), \ldots, r_{K,j}(\lambda_N)) && \text{(8d)} \end{aligned}$$

where the subindex $C$, $M$, $Y$, or $K$ represents the reflectance obtained in response to digital control values of the form $(C, 0, 0, 0)$ (cyan only), $(0, M, 0, 0)$ (magenta only), $(0, 0, Y, 0)$ (yellow only), or $(0, 0, 0, K)$ (black only), respectively. The subindex $j$ is an integer that denotes the experiment number and it runs from 1 to $Q$.

*Responses to multicolorant inputs:* To obtain a good representation of the input color space, colors combining $C$, $M$, $Y$ and $K$ are also included. The measured output reflectance sequences of these colors are denoted by

$$r_j = (r_j(\lambda_1), \ldots, r_j(\lambda_N)) \tag{9}$$

where $j = 1, \ldots, L$, with $L$ denoting the number of multicolorant experiments.

*Error bounds:* The error bound sequences are denoted by

$$\sigma_j = (\sigma_j(\lambda_1), \ldots, \sigma_j(\lambda_N)) \tag{10}$$

where the subindex $j$ indicates the reflectance sequence under consideration; see also equation (4).

### B. The Robust Estimation Algorithm (REA)

The algorithm proposed in [8] and [9] to estimate the dot growth functions, the corrected primary reflectances and the Yule-Nielsen correction factor $n$ is as follows.

*Initialization:* Fix the primary reflectances to the measured sequences (7). Fix a value for the Yule-Nielsen correction factor $n$. Compute initial values for the $Q$ samples of the dot-growth functions $C \mapsto c$, $M \mapsto m$, $Y \mapsto y$, $K \mapsto k$ by calculating the non-dimensional areas $c_1^*, c_2^*, \ldots, c_Q^*$; $m_1^*, m_2^*, \ldots, m_Q^*$; $y_1^*, y_2^*, \ldots, y_Q^*$; $k_1^*, k_2^*, \ldots, k_Q^*$, from the following scalar optimization problems,

$$\begin{aligned} c_\ell^* &= \arg \min_{c_\ell \in [0,1]} \| \, |\hat{r}_{C,\ell} - r_{C,\ell}| + \sigma_\ell \|_2 && \text{(11a)} \\ m_\ell^* &= \arg \min_{m_\ell \in [0,1]} \| \, |\hat{r}_{M,\ell} - r_{M,\ell}| + \sigma_\ell \|_2 && \text{(11b)} \\ y_\ell^* &= \arg \min_{y_\ell \in [0,1]} \| \, |\hat{r}_{Y,\ell} - r_{Y,\ell}| + \sigma_\ell \|_2 && \text{(11c)} \\ k_\ell^* &= \arg \min_{k_\ell \in [0,1]} \| \, |\hat{r}_{K,\ell} - r_{K,\ell}| + \sigma_\ell \|_2 && \text{(11d)} \end{aligned}$$

where $\hat{r}_{C,\ell}$, $\hat{r}_{M,\ell}$, $\hat{r}_{Y,\ell}$, and $\hat{r}_{K,\ell}$, for $\ell = 1, \ldots, Q$, are the model output reflectance sequences and $r_{C,\ell}$, $r_{M,\ell}$, $r_{Y,\ell}$, and $r_{K,\ell}$ are the measured reflectance sequences corresponding to single colorant inputs defined in (8).

*Main step:*

1) Fix the primary reflectances to the current guess. Refine the estimation of the dot-growth functions $C \mapsto c$, $M \mapsto m$, $Y \mapsto y$, $K \mapsto k$ by calculating the non-dimensional areas $c_1^*, c_2^*, \ldots, c_Q^*$; $m_1^*, m_2^*, \ldots, m_Q^*$; $y_1^*, y_2^*, \ldots, y_Q^*$; $k_1^*, k_2^*, \ldots, k_Q^*$, from the following scalar minimax optimization problems,

$$\begin{aligned} c_\ell^* &= \arg \min_{c_\ell \in [0,1]} \max_{j \in \Omega_{c_\ell}} \| \, |\hat{r}_j - r_j| + \sigma_j \|_2 && \text{(12a)} \\ m_\ell^* &= \arg \min_{m_\ell \in [0,1]} \max_{j \in \Omega_{m_\ell}} \| \, |\hat{r}_j - r_j| + \sigma_j \|_2 && \text{(12b)} \\ y_\ell^* &= \arg \min_{y_\ell \in [0,1]} \max_{j \in \Omega_{y_\ell}} \| \, |\hat{r}_j - r_j| + \sigma_j \|_2 && \text{(12c)} \\ k_\ell^* &= \arg \min_{k_\ell \in [0,1]} \max_{j \in \Omega_{k_\ell}} \| \, |\hat{r}_j - r_j| + \sigma_j \|_2 && \text{(12d)} \end{aligned}$$

where $\Omega_{c_\ell}$, $\Omega_{m_\ell}$, $\Omega_{y_\ell}$, and $\Omega_{k_\ell}$ denote the sets of experiments from (8) and (9) with control values fixed, respectively, at $C = C_\ell$, $M = M_\ell$, $Y = Y_\ell$, and $K = K_\ell$.

2) Set the dot-growth functions to the ones computed in step 1 and compute $N$ samples of the corrected primary reflectances by solving

$$\begin{aligned} &[\hat{r}_{P,1}^*, \ldots, \hat{r}_{P,16}^*] = \\ &\qquad \arg\min \max_j \| \, |\hat{r}_j - r_j| + \sigma_j \|_2 \qquad \text{(13)} \\ &\qquad \text{s.t. } |\hat{r}_{P,i}(\lambda_k) - r_{P,i}(\lambda_k)| \le \sigma(\lambda_k), \\ &\qquad i = 1, \ldots, 16, \quad k = 1, \ldots, N \end{aligned}$$

where $\hat{r}_j$ is the model output reflectance, which depends on the unknown primary reflectances $\hat{r}_{P,1}, \ldots, \hat{r}_{P,16}$. In (13), $r_j$ is the measured reflectance corresponding to single or multicolorant responses in (8) or (9), respectively, and $\sigma_j$ is the error bound corresponding to the measured reflectance $r_j$.

The main step may be iterated to obtain improved parameter estimates. Also, both the initialization and the main step need to be executed for a range of values of the Yule-Nielsen correction factor $n$ to identify the best one. The minimization problems in main steps 1 and 2 can be solved using functions from the Matlab Optimization Toolbox [13]. Further details may be found in [8] and [9].

## IV. Case Study

This section describes the performance of several spectral Neugebauer models for a high-end color printer. The models were obtained using three different methods, the robust estimation algorithm (REA), the least squares (LS) algorithm and the total least squares (TLS) algorithm. The LS and TLS algorithms are from [1]. For each method, the models were constructed using training data sets with increasing number of reflectances. The study has two main objectives: the first one is to compare the approximation errors of REA, LS, and TLS, and the second one is to investigate the variation of approximation errors with the size of the training set.

### A. The Experimental Data

The three data sets used for parameter estimation are the following. **Training set 1:** Single colorant reflectances of the form (8) obtained with $Q$=17 digital control values for each input, totaling 68 reflectances. **Training set 2:** Training set 1 plus 17 gray reflectances obtained with $C = M = Y$ and $K = 0$. **Training set 3:** Training set 2 plus 68 multicolorant reflectances of the form (9) obtained with $L = 17$ values of each single digital control input with the remaining digital control inputs set to mid-range.

In addition, the responses to 16 control values corresponding to the primary reflectances in equation (7) are used to initialize the algorithms.

**Test set:** This data is used for model validation and consists of $125$ control values taken from a homogeneous $5\times5\times5$ grid in the $CMY$ color space and converted to the $CMYK$ color space using a standard undercolor removal algorithm.

All printed patches were measured at four different spatial locations on the charts. Reflectances were measured at 10nm intervals between 380nm and 730nm using a Gretag spectrophotometer model SPM50. The reflectances used for parameter estimation and model validation were obtained averaging the four measurements available for each control value.

The error bound sequences $\sigma_j$ defined in (10) are required to implement the REA. These sequences have been estimated considering identical error bounds for all the reflectances; i.e., $\sigma_j = \sigma$ for all $j$. To determine the sequence $\sigma$ the four measurements available per control input in the training set were used. The mean of each four-measurement group was removed from the measured reflectances and the error bound sequence $\sigma$ was taken to be twice the standard deviation of the resulting data.

### B. Analysis of the models

Nine models were computed, 3 LS models, 3 TLS models, and 3 REA models. The LS and TLS models were obtained by applying the algorithms in [1] to the three data sets individually. The three REA models were obtained by applying two iterations of the algorithm described in section III-B to the three training sets. All the models were computed with Yule-Nielsen factor $n = 7$.

*Worst-case approximation errors over the training sets:* The distribution of the worst-case errors over the three training sets were calculated for each model. Specifically, for each of the nine models, the worst-case approximation errors $E_{\text{worst}}$ were calculated from equation (5) with the reflectances in the training set used to estimate the parameters of the model under consideration. Figure 2 shows two indicators of the magnitude of the worst-case errors, the largest worst-case error in the distribution (top plot), and the mean value of the distribution. This figure also shows the standard deviation of the worst-case error distribution. Notice that the largest worst-case error is exactly the cost function in equation (6) that REA seeks to minimize. For this reason, as shown in the top plot, these errors are minimal with REA for all three training sets. Notice also that the largest and mean values of the worst-case error distributions increase as experiments are added to the training sets. This is explained, in part, by the fact that the training sets are used for evaluation also, which in turn implies that the largest worst-case error will increase as experiments are added. It is interesting to note that the worst case errors (largest and mean values) with REA exhibit the smallest growth rate as experiments in the training set are included. This result suggests that REA is the least sensitive method to the variations in the training sets. This conclusion is also supported by the standard deviation plots, which show that REA achieves the smallest dispersions regardless of the training set.

*Worst-case approximation errors over the test set:* The distribution of the worst-case errors $E_{\text{worst}}$ of each model was also calculated over the test set. This allows to compare the worst-case behavior of the models using validation data which was not used for parameter estimation. In this analysis, the worst-case error distributions were evaluated using the same test data set for all nine models. Figure 3 shows the largest and mean values, and the standard deviation, of the worst-case error distributions. Notice that the worst-case errors (largest value or mean) tend to decrease as more experiments are used to train the models. This behavior, which holds for LS, TLS, and REA, is also intuitive as more, properly chosen, samples in the training set generally achieve lower approximation errors in the test set. The variations across models are not significant. However, REA achieves the best overall result; i.e., the smallest worst-case errors (largest or mean value) are obtained with REA and training set 3. Notice also that REA achieves the lowest standard deviations also.

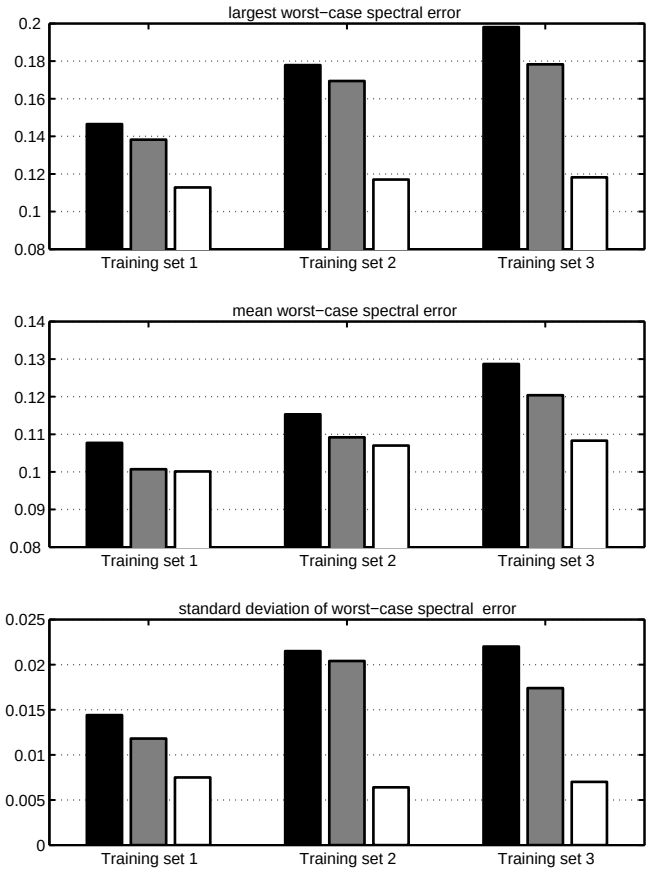


Fig. 2. Comparison of the largest value, mean value, and standard deviation of the worst-case error distributions with the training sets used for estimation. Black: LS, Gray: TLS, White: REA.

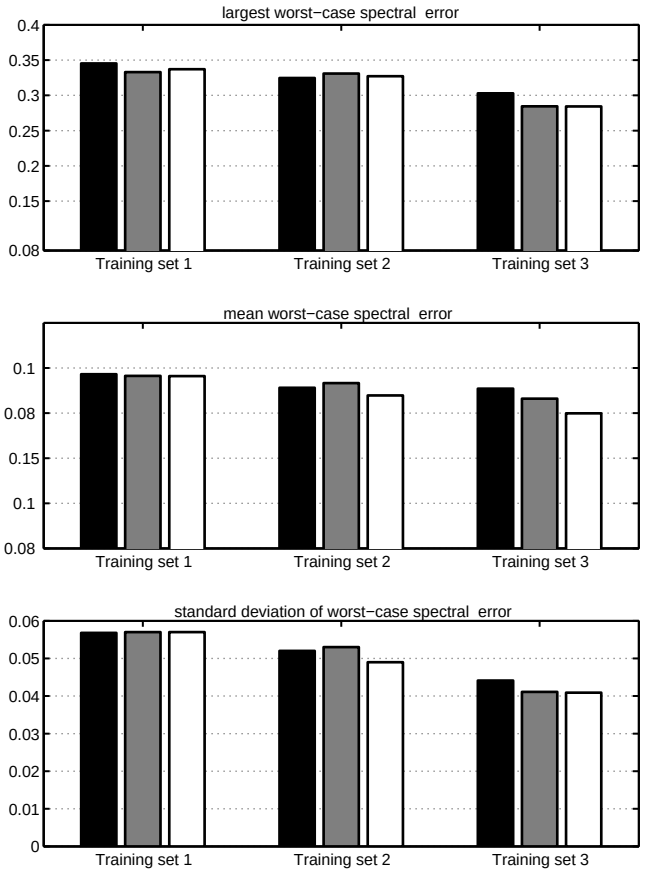


Fig. 3. Comparison of the largest value, mean value, and standard deviation of the worst-case error distributions with the test set. Black: LS, Gray: TLS, White: REA.

*Approximation errors in L*a*b* color space:* Approximation errors were also computed in the $L^*a^*b^*$ color space[1] using the color difference metric $\Delta E^*_{ab}$ [14]. This analysis used two data sets for all the nine models: training set 3 and the test set. The $\Delta E^*_{ab}$ error distributions were generated as follows. For each control value in the training set 3, 1000 reflectances were randomly generated using a normal distribution with mean equal to the average reflectance measurement, for that control value, and standard deviation equal to $\sigma/2$. A similar process was used to generate 1000 random reflectances for each control value in the test set. These random reflectances were converted to $L^*a^*b^*$ color space to generate 1000 "$L^*a^*b^*$ measurements" for each particular control input. The resulting "$L^*a^*b^*$ measurements" were then compared with the $L^*a^*b^*$ color output of each model[1], using the color difference metric $\Delta E^*_{ab}$. Hence, for each control value $CMYK$, there are 1000 values of $\Delta E^*_{ab}$, which are classified into training set 3 and test set, depending on the particular control value used.

Figure 4 shows the mean and the standard deviation of the $\Delta E^*_{ab}$ error distribution from training set 3. The three methods exhibit the same trend as additional experiments are incorporated in the data sets used to train the models. In most cases, the mean approximation error decreases with the number of experiments used in the training set. The variation amongst the models is not significant. However, REA achieves the best overall result when used on training set 3; i.e, the model obtained with REA has the lowest average $\Delta E^*_{ab}$ with the lowest standard deviation. It is important to remark that REA does not minimize the mean approximation error in $L^*a^*b^*$ color space; hence, the REA-based model is not optimal under this measure of performance. Figure 5 shows the mean and the standard deviation of the $\Delta E^*_{ab}$ error distribution from the test set. The results are similar to the ones in Fig. 4. The main difference is that the models obtained with REA achieve the lowest average approximation errors and standard deviations for all the cases.

[1]Reflectances are converted to $L^*a^*b^*$ color space under the CIE illuminant D50.

## V. Conclusions

A robust algorithm (REA) to estimate the device-specific parameters of the so-called spectral Neugebauer model was described. This algorithm is based on the idea that the most robust set of parameters is the one that minimizes the largest

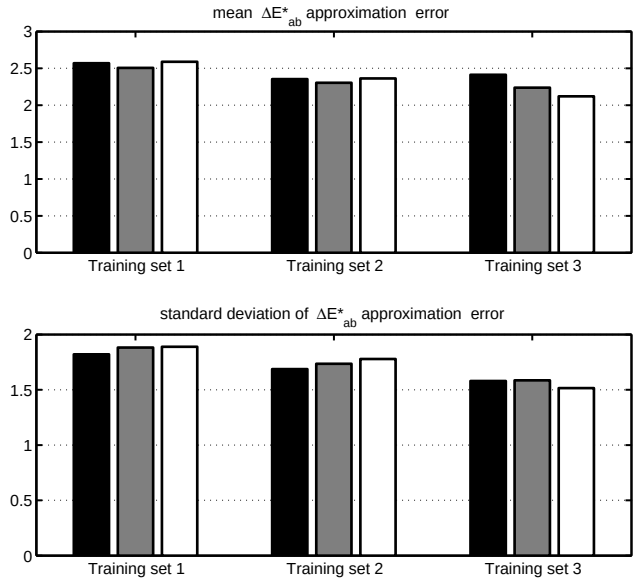


Fig. 4. Comparison of the mean and standard deviation of the approximation error distributions in $L^*a^*b^*$ color space with the training set 3. Black: LS, Gray: TLS, White: REA.

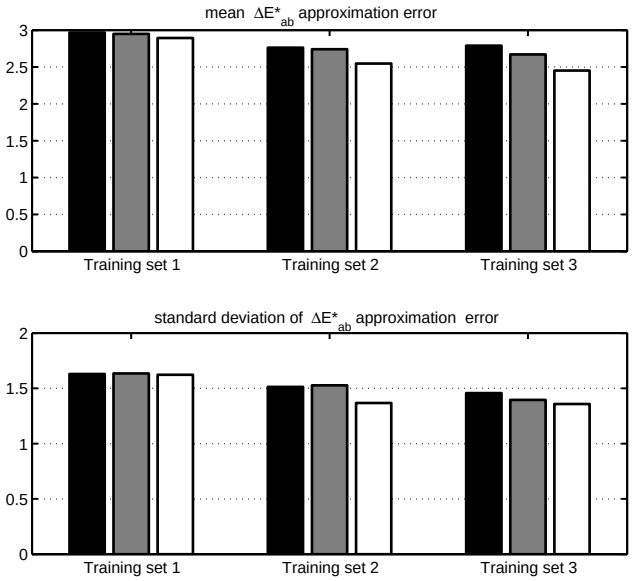


Fig. 5. Comparison of the mean and standard deviation of the approximation error distributions in $L^*a^*b^*$ color space with the test set. Black: LS, Gray: TLS, White: REA.

worst-case spectral approximation error over the entire set of training experiments. This minimization problem is not convex and hard to solve. REA gives a suboptimal solution to this problem by splitting it into two simpler subproblems, the estimation of dot growth functions and the estimation of the corrected primary reflectances.

The results of a case study using a high-end color printer were given. The analysis of approximation errors in spectral space showed that REA is capable of producing distributions of the worst-case approximation error with the smallest values (max and mean), and the least dispersion (Fig. 2). Hence, the models obtained with REA achieve the best performance, uniformly over the various training sets. Further analysis with test data, not used for parameter estimation, showed comparable performance for all the three methods, LS, TLS and REA. However, the model obtained with REA and training set 3 showed the best performance amongst all nine models (Fig. 3). This conclusion also holds true when the models are evaluated in the $L^*a^*b^*$ color space (Figs. 4 and 5).

## REFERENCES


[1] M. Xia, E. Saber, G. Sharma, and M. Tekalp, "End-to-end color printer calibration by total least squares regression," *IEEE Transactions on Image Processing*, vol. 8, no. 5, pp. 700–716, May 1999.

[2] P. Emmel and R. Hersch, "Colour calibration for colour reproduction," in *IEEE International Symposium on Circuits and Systems*, Geneva, Switzerland, May 2000, pp. V105–V108.

[3] P. C. Hung, "Colorimetric calibration in electronic imaging devices using a look-up table model and interpolations," *Electronic Imaging*, vol. 2, pp. 53–61, January 1993.

[4] J. Hardeberg and F. Schmitt, "Color printer characterization using a computational geometry approach," in *IS&T and SID's 5th Color Imaging Conference: Color Science, Systems and Applications*, 1997.

[5] R. Balasubramanian, "The use of spectral regression in modeling halftone color printers," in *IST/OSA Anual Conference, Optics Imaging in the Information, Age Rochester, NY*, October 1996, pp. 372–375.

[6] ——, "Optimization of the spectral Neugebauer model for printer characterization," *Electronic Imaging*, vol. 8, no. 2, pp. 156–166, April 1999.

[7] R. Rolleston and R. Balasubramanian, "Accuracy of various types of Neugebauer models," in *IS&T and SID's Color Imaging Conference: Transforms and Transportability of Color*, Nov. 1993, pp. 32–37.

[8] C. Lana, M. Rotea, and D. Viassolo, "Characterization of color printers using robust parameter estimation," *Journal of Electronic Imaging, submitted for publication*, 2003.

[9] M. Rotea, C. Lana, and D. Viassolo, "Robust estimation algorithm for spectral Neugebauer models," in *Proceeding of the 42nd IEEE Conference on Decision and Control, Maui, Hawaii*, Dec. 2003, pp. 4109–4114.

[10] J. A. S. Viggiano, "Modeling the color of multi-colored halftones," in *Technical Association of the Graphic Arts (TAGA)*, 1990, pp. 44–62.

[11] ——, "The color of halftone tints," in *Technical Association of the Graphic Arts (TAGA)*, 1985, pp. 647–661.

[12] E. Demichel, *In Procédé*, vol. 26, pp. 17–21,26–27, 1924.

[13] MathWorks, *Optimization Toolbox User's Guide, version 2.1*, 2000.

[14] CIE, *Colorimetry*, 2nd ed., C. Publication, Ed. Central Bureau of the CIE, Vienna, Austria: CIE Publication no. 15.2, 1986.